16th European Signal Processing Conference (EUSIPCO 2008), Lausanne, Switzerland, August 25-29, 2008, copyright by EURASIP

A NEW GENERATION OF NON-INVASIVE BIOMARKERS OF COGNITIVE-MOTOR STATES WITH APPLICATION TO SMART BRAIN-COMPUTER INTERFACES

Rodolphe J. Gentili[1], Trent J. Bradberry[1,2], Bradley D. Hatfield[1,3], José L. Contreras-Vidal[1,2,3]

Department of Kinesiology[1], Fischell Department of Bioengineering[2], Neuroscience and Cognitive Science Program[3]
School of Public Health, University of Maryland, College Park, 20742, USA.
phone: + (1) 301-405-2495, fax: + (1) 301-405-5578, email: {rodolphe, trentb, bhatfiel, pepeum}@umd.edu
web: http://www.sph.umd.edu/KNES/ research/cmb.html

ABSTRACT

The design of assistive technologies such as non-invasive brain computer interfaces (BCI) requires an improved understanding of the cortical dynamics of the human brain when interacting with new tools and/or adapting to novel environments in ecological situations. Therefore the aim of this study was to investigate potential biomarkers able to reflect dynamic cognitive-motor states of subjects who had to learn a new tool. These biomarkers were derived from the power bands of electroencephalographic (EEG) signals. The EEG and hand kinematic signals were analyzed for subjects of a Learning Group (LG; n=10) who performed self-selected/initiated center-out hand movements during a visuomotor adaptation task. A Control Group (CG; n=5) was also tested with the same task; however, no adaptation was required. For the LG, the findings indicated that the alpha ([9-13] Hz) and high theta ([6-7] Hz) power computed at the frontal and temporal sites showed a consistent linear and bilateral increase during movement planning during tool learning that may represent the update of the internal model of the new tool. The power increases were correlated with enhanced kinematics as the task progressed. No such differences appeared for the CG. These non-invasive biomarkers appear able to track the human learning/adaptation status and may play a role to overcome specific pitfalls in BCI applications such as the need for frequent recalibrations and the management of the co-adaptation/cooperation between the user's brain and the decoding algorithm required to design the next generation of smart neuroprostheses.

1. INTRODUCTION

The restoration of cognitive-motor function (e.g. in disabled populations, advanced aging) and bioengineering applications, such as the design of smart neuroprosthetics, require a deeper understanding of brain dynamics in ecological situations that involve human interaction with new tools and/or changing environments that guide learning and more generally shape our motor behaviour. The assessment of such brain dynamic status necessitates the knowledge of new neural indicators or biomarkers which should be preferably non-invasive, simple to record and analyze, simultaneously robust and sensitive to changes in brain function in ecological situations. Nevertheless, until now, most studies aiming to identify brain biomarkers have mainly focused on biochemical, cellular, and genetic aspects related to brain disorders [1-2]. Although helpful, this approach is not suitable to provide direct indicators to assess the functional status of the brain [2]. This assessment is only possible through the use of appropriate methods for recording dynamic brain activity with a high (e.g. millisecond) temporal resolution, such as electroencephalography (EEG). More importantly, no biomarker of cognitive states during human sensorimotor learning is currently available. Therefore, the aim of this study was to investigate the presence of such biomarkers underlying the acquisition of the internal model of a new tool.

2. MATERIALS AND METHODS

Participants and apparatus

Fifteen right-handed healthy adults participated in the study after giving informed consent. All had normal or corrected-to-normal vision. Subjects sat at a table facing a computer screen and, with their right hand, had to perform "center-out" drawing movements on a digitizing tablet linking a central target and one of four peripheral targets. Movement paths were displayed on the screen, but a vertical board did not permit vision of the moving limb on the tablet (Fig.1). EEG signals were acquired using an electro-cap with 64 tin electrodes, which was fitted to the participant's head in accordance with the standards of the extended International 10-20 system. The EEG recording apparatus consisted of a Synamps acquisition system and Neuroscan v.4.1 software.

Experimental procedure

First, the subjects performed 20 practice trials at the beginning of the experiment in order to be familiarized with the experimental setup. After this familiarization period, the experiment was divided into three sessions: i) pre-exposure, ii) exposure and iii) post-exposure. During the pre- and post-exposure phases the subjects performed, under normal visual conditions, 20 trials (i.e. 1 block). During the exposure phase, (180 trials, i.e. 20 trials x 9 blocks) ten subjects (labeled *Learning Group* or *LG*) had to adapt to a 60º counter clockwise screen cursor rotation. In addition, five healthy (labeled *Control Group* or *CG*) subjects were examined using the same protocol but in the absence of any visual distortion. Movements were self-initiated and targets were self-selected one at a time. All the targets were displayed throughout each trial. The instructions were to draw a line as straight and as fast as possible linking the home target and the peripheral

target. Furthermore, subjects were instructed to avoid following any regular sequence in selecting targets. Unknown to the participants, a trial was aborted and restarted if the time between entering the home target and movement onset was less than 2s. Therefore, participants had enough time to both select the target and plan their movement thus providing an extended time-window to analyze cortical activations related to planning and preparation processes of the motion.

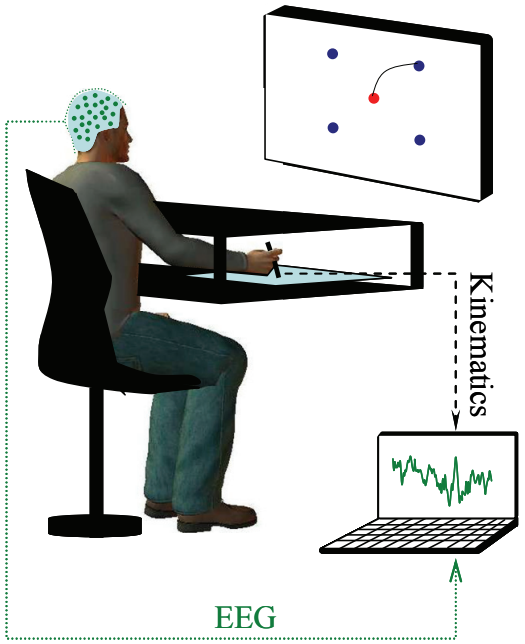

Figure 1 - Experimental device to record kinematics and EEG signals during the visuomotor adaptation task. Subjects sat at a table facing a flat computer screen located in front of them at a distance of approximately 60 cm and had to execute the motor task which consisted of drawing a line on a digitizing tablet (represented in light blue on the figure) that was displayed in real-time on the computer screen. The home target circle (Red, diameter 5 mm) was the origin of a direct polar frame of reference, and the target circles (Blue, diameter 5 mm) were positioned 10 cm from the origin disposed at 45°, 135°, 225°, and 315° from the origin. Once a successful trial was performed, to prevent any feedback, all visual stimuli were erased from the screen in preparation for the next trial. The duration between trials was self-paced by the subject but lasted at least 2s. To minimize fatigue and maintain attention, brief rest periods were allowed if needed. A chin rest and nose bridge head positioner (not shown here) was used to stabilize the participant's head in order to minimize muscle artifact.

Data analysis

Movement kinematics

The 2D displacements were low-pass filtered using a 5-Hz, eighth-order Butterworth filter. In order to quantify the motor performance during both movement planning and movement execution periods, the Movement Time (MT) and Movement Length (ML) were computed. The MT was defined as the elapsed time between leaving the home circle and entering the target. The ML was defined as the distance travelled in each trial. For the nine learning blocks, the mean and standard deviation of the ML and MT were computed. In order to take into account any differences in subject's performance during the pre-exposure phase (i.e. baseline condition) and to focus on changes due solely to adaptation, the MT and ML values were standardized with respect to the pre-exposure stage according to the following equation:

$$SP_i = \frac{P_i - \overline{P_{\mathrm{Pr}\_Exp}}}{SDP_{\mathrm{Pr}\_Exp}} \qquad (1)$$

where P_i (P: Parameter) is the value of the kinematic parameter (i.e. MT or ML) computed for the i^{th} single trial performed during the exposure, and $\overline{P_{\mathrm{Pr}\_Exp}}$ and SDP_{Pr_Exp} represent respectively the mean and standard deviation across trials of the same parameter computed during the pre-exposure block. The SP_i (SP: Standardized Parameter) values were then averaged across blocks and subjects. These average MT and ML standardized values were statistically tested using a *Wilcoxon signed rank test* to assess any changes between the early and late learning phase.

EEG preprocessing

Continuous EEG data were epoched in 2-s windows centered at movement onset. Only the pre-movement time-window (i.e. planning) was considered. Single-trial data were detrended to remove DC amplifier drift, low-pass filtered (below 40Hz) to suppress line noise, and baseline-corrected by averaging the mean potential from -1 to 1 s.

EEG power computation

For each subject and each single-trial, a band-pass fourth-order Butterworth filter was used to extract, from the EEG signal, eight frequency bands corresponding to the low (α_L: [8-10] Hz; β_L: [13-20] Hz; θ_L: [4-5] Hz) and the high (α_H: [11-13]; β_H: [21-35]; θ_H: [6-7] Hz) components of the alpha, beta, and theta bands. In addition, the frequency band spread from 9 to 13 Hz (alpha band) was also analyzed. This filter was applied forward and backward (i.e. dual-pass filtering) to avoid any signal distortion. For each band, the filter output was squared and integrated for each time-window to obtain the power for each frequency band and trial. For the same reasons as those previously mentioned and also to perform homogenous data processing for both kinematic and electrophysiological parameters, the computed power values were also standardized using equation (1). The only difference is that P_i represents the electrophysiological parameter, corresponding here to a given EEG power value, and SP_i represents the standardized power. The SP_i values were then averaged across blocks and subjects.

Curve fitting

For each sensor and each block, the average power changes (across subjects) were fitted using a linear model from which the coefficient of determination (R^2) and its slope were obtained. The sensors that showed a fit indicating a coefficient of determination capable to explain at least 50% of the variability of the data (i.e. $R^2 \geq 0.50$) allowed us to determine the sensor clusters and the frequency bands of inter-

est. The results of this procedure led us to consider the alpha frequency band and the high component of the theta frequency band for the right (FT8, T8, TP8) and left (FT7, T7, TP7) temporal and right (FP2, AF4, F4, F6, F8) and left (FP1, AF3, F7, F5, F3) frontal lobes. For these two bands and clusters of interest, the average power values were computed, and the same fitting process was applied. Furthermore, in order to investigate any correlation between the kinematics data and the EEG power, the MT and ML values were plotted versus the average EEG power obtained for the temporal and frontal clusters. Exponential (single and double), linear and quadratic models were used to fit these relationships. The best fit was selected by considering the coefficient of determination and its adjusted value, the Root mean square error of the Fit (RmseF), and the sum of squares due to the fitting error.

3. RESULTS

Overall, the results from the *LG* indicated that subjects showed consistent electro-cortical changes during the planning phase of hand movements in the alpha and (high) theta power EEG bands extracted from the temporal and frontal lobes. These electrophysiological changes were correlated to an enhancement of the kinematics throughout learning. Conversely, the subjects of the *CG* did not show similar changes.

Electrophysiogical results

The four clusters computed from the *LG* covering the right and the left frontal lobes showed a consistent linear increase in both alpha and high theta power throughout the exposure (distorted) trials during the planning stage. Contrary to the *LG*, the subjects of the *CG* did not show any linear power changes in the alpha and theta frequency bands for either frontal or temporal lobes (compare the blue and black plot in Fig.2A and 2B). Moreover, while the subjects of the *LG* also indicated linearly increasing, bilateral alpha power in the temporal clusters, the same brain region of the *CG* did not exhibit such tendency. On the contrary, the alpha power even tended to decrease (compare the blue and black plot in Fig.2D). Finally, the subjects of the *LG* indicated a consistent linear increase in theta power only in the left temporal clusters, but the CG did not even though the power values were relatively close (Fig.2C, left panel). For the right temporal cluster, no difference appeared between the LG and CG (see Fig.2C right panel). More specifically, for both left and right temporal and frontal lobes, all slopes obtained for the *LG* (i.e. when $R^2 \geq 0.5$) in the alpha band were statistically different from zero (two-tailed *t-test*) and also differed between the *LG* and the *CG* ($p<0.001$). Furthermore, the LG showed that for the high theta power band, the slopes obtained for the frontal lobes and the left temporal lobes were different from zero ($p<0.01$). Using the same analysis, the linear model could not fit the power values for the *CG* ($R^2 \leq 0.13$). At last, the average power values for both alpha and theta bands decreased from the last learning block to the first trials of the post-exposure (i.e. the subject perform poorly since the perturbation was removed) and then increased again once the original tool was reacquired after few trials.

Kinematic results

For the subjects of the *LG*, a sudden introduction of the rotational perturbation caused distorted movement trajectories and slow progression towards the targets during the early exposure phase; however, as the training progressed, these trajectories became straighter and smoother indicating that the subjects were learning the internal model of the novel visuomotor perturbation (i.e., new tool) [3].

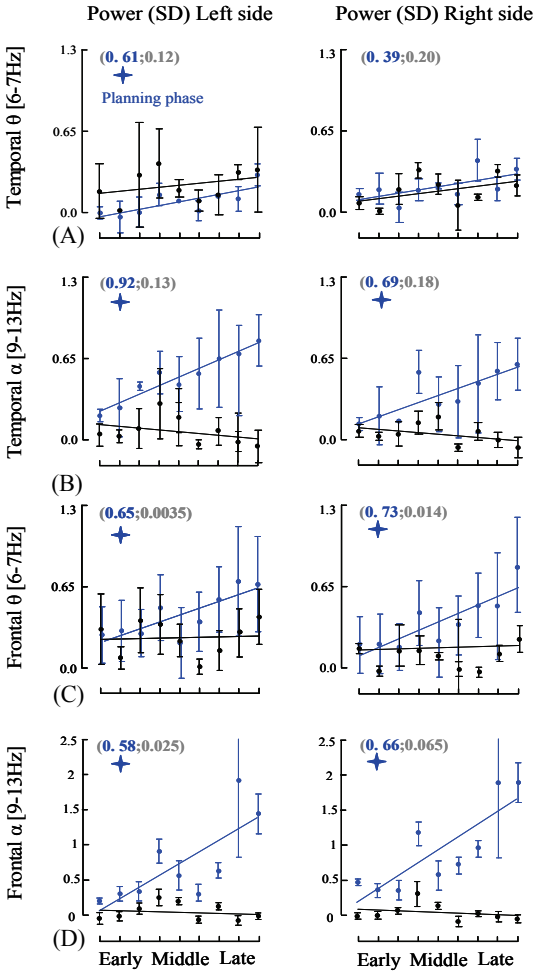

Figure 2 - Linear increase in alpha (α) and theta (θ) power for the left (first column) and right (second column) frontal (two first rows) and temporal (two last rows) lobes and for the *LG* (plotted in blue) and the *CG* (plotted in black) throughout the early, middle and late learning stages. Numbers between brackets represents the coefficient of determination (R^2) for each group whereas the blue star indicates that the slopes computed were significantly different from zero for the *LG*. Note that the scale displayed in the last row is different from that used in the three first rows.

Such behavioural enhancement was reflected by the MT and ML, which exhibited significantly higher values during the early exposure phase than the late exposure phase (*Wilcoxon test*, $p<0.0013$). In contrast to the *LG*, as expected, the CG did not show any quantitative or qualitative kinematic improvement (*Wilcoxon test,* $p>0.05$, for both MT and ML). For the two groups, these kinematics findings are illustrated in Fig. 3A (compare the right and left column).

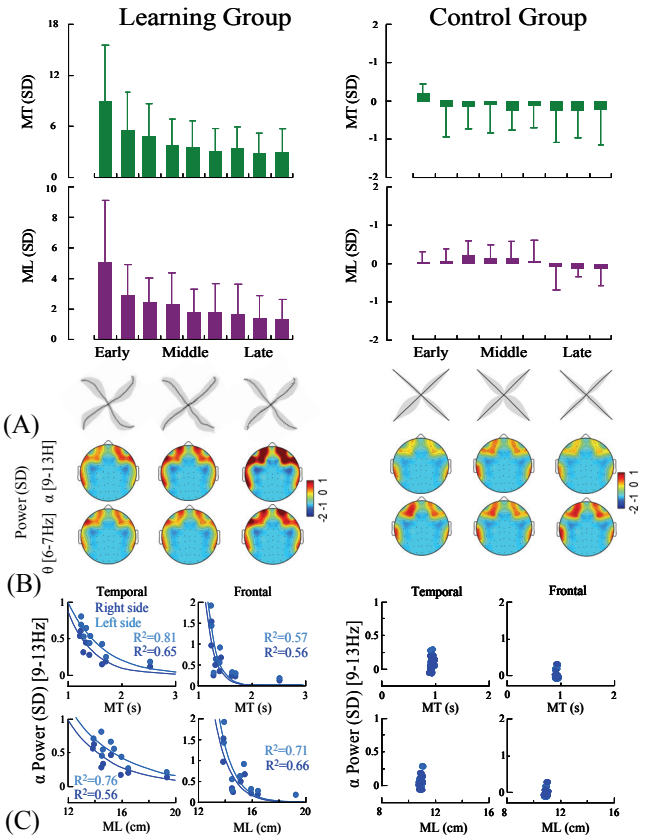

Figure 3 – A. Standardized values of MT (first row, green) and ML (second row, purple) for the *LG* (first column) and *CG* (second column). The third row represents the trajectories produced by the subjects throughout the learning phase. B. Scalp plot representing power changes for the clusters of interest in the alpha (α; [9-13Hz]) and theta frequency (θ; [6-7Hz]) bands for the *LG* (left column) and the *CG* (right column). C. Representation of the EEG standardized power in the alpha (α) frequency band versus the MT (first row) and the ML (second row) changes for the right (dark blue) and the left (clear blue) temporal and frontal clusters. For each panel and for each right and left cluster, the curves representing the best fit (i.e. single exponential) for each relationship for the *LG* (two first columns) and CG (two last columns) are illustrated with the coefficient of determination (R^2) representing the quality of the fit.

Specifically, throughout training, the bilateral increase in alpha and high theta EEG power in the frontal and left temporal lobes during movement planning were accompanied by concurrent changes in the trajectories and associated kinematic parameters (MT, ML) for the *LG*. No such changes were visible at the kinematic or electrophysiological levels of the *CG*. These differences are particularly visible when comparing the third row of Fig. 3A (the trajectories) and Fig. 3B (i.e. scalp plot) for the *LG* (left column) with the same data obtained from the *CG* (right column).

Correlation and fitting analyses

The results for the fitting and correlation analyses showed that the relationships between the increased alpha power values for the left and right temporal and frontal clusters and the MT and ML values were best fitted by using a single exponential ($R^2 \geq 0.56$, RmseF<0.42).

4. DISCUSSION

The main findings of this study are that the *LG* showed linear and bilateral EEG alpha and high theta increases in power in the temporal and frontal lobes during movement planning, and that such increases were correlated with enhanced kinematics throughout visuomotor learning. Conversely, the findings for the *CG* demonstrated that the kinematic and electrophysiological parameters in the same center-out movement task remained unchanged (or steady state) when no visual distortion had to be learned.

Such frontal and temporal EEG power changes mirroring human motor performance may provide potentially powerful biomarkers for tracking human learning/adaptation status when one has to learn/adapt to a new tool. Therefore, they could play a significant role in a broad range of applications related to brain monitoring and cognitive-motor status assessment. One of the main roles of these biomarkers would be to overcome the widely admitted [4-5] difficulties in brain-computer interface (BCI) systems such as adaptive decoding, constant recalibration and the maintenance of stable performance while a user tries to control a neuroprosthesis. Traditionally, motor-imagery-based BCI approaches are divided into two phases. The first one consists of a calibration phase to determine the parameters of a decoding algorithm, which has to map neural signals to a class of imagined movement. The second phase aims to train the subject by providing him/her sufficient feedback to change his/her cortical dynamics in order to control an external device via the BCI system. It is important to note that during this second stage, since the adaptation depends on the capacity of the user's brain to change its cortical dynamic, frequent recalibrations of the decoding algorithms are required when the user's performance degrades [4-5]. This important drawback of BCI's could be solved by the type of biomarkers that we investigated in the present study. Indeed, such biomarkers could be used to continuously adapt the decoding algorithm to the subject's mental states, thereby allowing a stable co-adaptation/cooperation between the user and the BCI system. This is especially relevant when the user has to learn the physical properties of a new tool and/or a novel environment. For example, if the user's brain considerably adapts as indicated by an increased alpha and/or theta power, the algorithm should not update its parameters. Conversely, it should adjust the parameters in order to compensate for a user's poor performance.

The complexity of using two adaptive controllers (the user's brain and the decoding algorithm) is not new and has been already raised by [6]; however, it continues to be an issue, and no satisfying solutions of this problem have been provided [7]. So far, the adaptive algorithms proposed to address this problem [8-9] use supervised adaptation relying on the knowledge of an external target. Although helpful, the requirement of such *a priori* information actually represents a major pitfall for practical BCI applications since the user should decide when and where to direct his/her intentions. In other words, no information of external targets is available to the decoding algorithm [10-11]. Nevertheless, the biomarkers evidenced here offer a new possibility to overcome such a

difficulty since they can be used as reinforcement signals to guide the decoding process. For instance, the power in the high theta and/or alpha frequency bands could be computed using a sliding window (e.g., 15-20 trials) applied to the sensors of the temporal and frontal lobes. Thus, if this power decreases (i.e. a poor performance of the user) the decoding algorithm should update its parameters (using for instance reinforcement learning), conversely, if the power increased no changes would be needed.

Importantly, the use of such biomarkers could also reveal sources of alterations in behavioural performance, which cannot be revealed by kinematics parameters alone. For instance, in our study, the absence of learning/adaptation could also be due to fatigue; however, the frontal biomarkers evidenced here are neither in the same spatial location (frontal midline) nor in the same frequency band (low theta band) than the fatigue-related EEG power [12]. Therefore, these features would also be able to monitor and fit the training time-scale for each individual while also allowing the algorithm to adapt to the user's cognitive state, which is usually impossible to access through behavioural measures. For example, for a practical use, it is important to decipher if a user's poor BCI performance is related to fatigue or to bottlenecks related to information processing resulting in poor performance.

Finally, it must be noted that the simplicity of the computational method presented in this report could also be transferable to hardware implementation at the chip-level for a wireless EEG system and is therefore well suited for online BCI control and more generally for dynamic brain monitoring in practical/ecological applications. However, additional future research is needed to obtain a more comprehensive knowledge of these biomarkers in order to clarify, for instance, if they will be reliably detectable and applicable under covert motion execution with an actual BCI closed-loop set-up or how their processing can be affected by individual specificities (e.g. different motor disabilities or aging) of potential BCI users.

5. CONCLUSION

The reported non-invasive biomarkers of learning computed while a human subject had to learn a new tool appear promising to solve various problems encountered in BCI designs such as frequent recalibration and co-adaptation/cooperation between the user's brain and the decoding algorithm. More generally, they appear capable of deciphering cognitive-motor mental states of human sensorimotor learning/adaptation and appear well suited for brain monitoring and cognitive-motor status assessments in early diagnosis in subject's performance, physical rehabilitation and in the design of the next generation of smart neuroprosthesis.

6. AKNOWLEDGEMENTS

La Fondation motrice (Paris, France).
Association Française contre les Myopathies (Paris, France).

REFERENCES

[1] E. K. Ryu and X. Chen, Development of Alzheimer's disease imaging agents for clinical studies. *Front Biosci.* 1; 13:777-89, Jan. 2008.

[2] A. P. Georgopoulos, E. Karageorgiou, A. C. Leuthold, S. M. Lewis, J. K. Lynch, A. A. Alonso, Z. Aslam, A. F. Carpenter, A. Georgopoulos, L. S. Hemmy, I. G. Koutlas, F. J. Langheim, J. R. McCarten, S. E. McPherson, J. V. Pardo, P. J. Pardo, G. J. Parry, S. J. Rottunda, B. M. Segal, S. R. Sponheim, J. J. Stan wyck, M. Stephane, J. J. Westermeyer, Synchronous neural interactions assessed by magnetoencephalo graphy: a functional biomarker for brain disorders, *J Neural Eng.* 4(4):349-55, Dec. 2007.

[3] J. L. Contreras-Vidal and S. E. Kerick, Independent com ponent analysis of dynamic brain responses during visuomotor adaptation, *Neuroimage*, 21(3): 936-945, Mar. 2004.

[4] W. Klimesch, B. Schack and P. Sauseng, The functional significance of theta and upper alpha oscillations, *Exp Psychol.,* 52(2):99-108, 2005.

[5] G. Pfurtscheller, C. Neuper, D. Flotzinger, M. Pregenzer, EEG-based discrimination between imagination of right and left hand movement, *Electroencephalogr Clin Neurophysiol.,* 103:642-51, Dec. 1997.

[6] T. M. Vaughan, J.R. Wolpaw, E. Donchin, EEG-based communication: prospects and problems. *IEEE Trans Rehabil Eng. 4:*425-30, Dec. 1996.

[7] D. J. McFarland, C. W. Anderson, K. R. Muller, A. Schlogl, D. J. Krusienski, BCI Meeting 2005–workshop on BCI signal processing: feature extrac tion and translation, *IEEE Trans Neural Syst Reha bil Eng.,* 14:135-8, Jun. 2006.

[8] P. Sykacek, S. J. Roberts, M. Stokes, Adaptive BCI based on variational Bayesian Kalman filtering: an em pirical evaluation, *IEEE Trans Biomed Eng.* 51:719-27, May 2004.

[9] B. Blankertz, K.R. Muller, D. J. Krusienski, G. Schalk, J. R. Wolpaw, A. Schlogl, G. Pfurtscheller, J. R. Mil lan, M. Schroder, N. Birbaumer, The BCI compete tion. III: Validating alternative approaches to actual BCI problems, *IEEE Trans Neural Syst Rehabil Eng.* 14:153-9, Jun. 2006.

[10] T. M. Vaughan, W. J. Heetderks, L. J. Trejo, W. Z. Ry mer, M. Weinrich, M. M. Moore, A. Kubler, B. H. Dobkin, N. Birbaumer, E. Donchin, E. W. Wolpaw, and J. R. Wolpaw, Brain-computer interface tech nology: a review of the Second International Meet ing, *IEEE Trans Neural Syst Rehabil Eng.,* 11:94-109, Jun. 2003.

[11] C. Vidaurre, A. Schlogl, R. Cabeza, R. Scherer, G. Pfurtscheller, Study of on-line adaptive discriminant analysis for EEG-based brain computer interfaces, *IEEE Trans Biomed Eng.,* 54:550-6, Mar. 2007.

[12] S. Makeig, T. P. Jung, T. Sejnowski, Awareness during drowsiness: dynamics and electrophysiological cor relates, *Can J Exp Psychol* 54, pp. 266–273, Dec. 2000.